# Hierarchical Nanoflake Surface Driven by Spontaneous Wrinkling of Polyelectrolyte/Metal Complexed Films

**Young Hun Kim,[†] Yong Man Lee,[‡] Jun Young Lee,[†] Min Jae Ko,[§] and Pil J. Yoo[†,‡,*]**

[†]School of Chemical Engineering and [‡]SKKU Advanced Institute of Nanotechnology (SAINT), Sungkyunkwan University, Suwon 440-746, Republic of Korea and [§]Solar Cell Center, Korea Institute of Science and Technology (KIST), Seoul 136-791, Republic of Korea

**ABSTRACT**

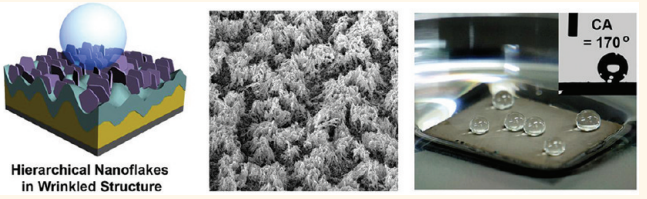


**A mechanical or physical change observed in nanocomposite thin films has recently offered new opportunities to generate intriguing nanostructures. In this study, we present a novel means of creating a hierarchically developed nanoflake structure by exploiting surface wrinkles that occur during the incorporation process of metallic nanoparticles into layer-by-layer assembled polyelectrolyte multilayer (PEM) thin films. The PEM film composed with linear polyethylenimine (LPEI) and poly(acrylic acid) (PAA) allows for facilitated cationic exchange reaction within the film even after the electrostatic complexation and chemical cross-linking reaction. The subsequent reduction process induces an *in situ* complexation of metallic nanoparticles with a PEM matrix, causing an accumulation of lateral compressive stress for surface wrinkling. The wrinkling characteristics of the complexed films can be theoretically interpreted by employing the gradationally swollen film model, whereby a gradual change in the elastic property along the axial direction of the film can be appropriately reflected. In addition, wrinkled surfaces are further processed to form vertically aligned and hierarchically ordered nanoflakes after selective removal of the PEM matrix with plasma ashing. Consequently, superhydrophobic surface properties (water contact angle = 170°, sliding angle <1°) can be attained from the hierarchical nanoflake structure. The method presented here is advantageous in that large-scale preparation can be readily implemented by a stepwise dipping process without resorting to specific patterning or a serially applied complex structuring process, which can provide a promising platform technique for various surface engineering applications.**

**KEYWORDS:** hierarchical nanostructures · wrinkling · layer-by-layer assembly · polyelectrolyte multilayers · superhydrophobic surface

Motivated by interesting biological surfaces observed in nature, researchers have extensively investigated hierarchical nanostructures by presenting various biomimetic systems.[1,2] Hierarchical nanostructures have helped to create outstanding physicochemical properties over a large scale, leading to a broad range of applications in surface chemistry,[3] optical structures,[4] or biomedical devices.[5] Recent studies have suggested applications for high capacity energy devices based on the utilization of their structural characteristics, with which maximized surface area and highly interconnected structures could be achieved.[6−8] While such hierarchical nanostructures have received much attention due to exquisite structural controllability and superior physical properties, they also have the disadvantages of requiring a complex fabrication process, such as high-resolution photolithography or intricate chemical synthesis.

As an alternative to overcome this drawback, a means to form spontaneous structures has been attempted, wherein various physical interactions are directly harnessed to generate hierarchical nanostructures.[9] Representative examples include interfacial self-assembly of micro- or nanodroplets or capillarity-driven construction of hierarchical structures.[10,11] The surface wrinkling phenomenon is another case of spontaneous structure formation.[12,13] When a stacked multilayer film comprising materials with different mechanical properties is placed in a mechanically unstable condition, compressive stress subsequently accumulates within the film. If the magnitude of this stress exceeds the critical value, spontaneous surface wrinkling occurs to reduce the system's energy. The resulting wrinkled structures can be manipulated to hierarchical structures according to the magnitude or duration of the applied compressive stress.[14,15]

Alternatively, layer-by-layer (LbL) assembled polyelectrolyte multilayer (PEM) film is capable of creating a spontaneous wrinkling phenomenon.[16] Polyelectrolyte multilayer films can be constructed *via* sequential depositions between oppositely charged polyelectrolyte chains, wherein the electrostatic interactions are elaborately

* Address correspondence to pjyoo@skku.edu.

Received for review August 22, 2011 and accepted January 2, 2012.

**Published online January 11, 2012**
**10.1021/nn203226k**

manipulated to control the thickness, composition, or internal structure of the assembled film. Due to the robustness and large-scale applicability of the LbL assembly process, PEM films have been widely used for various applications.[17] Notably, PEM films can also bring about surface wrinkles in response to environmental changes, such as thermal or swelling-induced expansion of the films. Since the assembled films are tightly bound to the underlying substrate, a strong compressive stress is generated as a counterbalanced response to the film expansion, yielding surface wrinkling. Due to the random and disordered structures of surface wrinkles, previous research on PEM wrinkling has focused on instability analysis to suppress the occurrence of wrinkling in the system.[18,19] Recently, however, beneficial aspects of PEM wrinkling have been exploited in practice for a novel metrology of measuring the mechanical properties of the PEM thin films or to create complex patterned and ordered wavy structures.[20−22] Nevertheless, large-scale hierarchical structuring of wrinkled PEM films has not yet been explored.

In this study, we present a novel means of generating and controlling the hierarchically wrinkled structures on polyelectrolyte multilayer surfaces. To induce surface wrinkling, Ag nanoparticles are incorporated into chemically cross-linked yet water-swollen PEM films by means of cationic exchange and subsequent reduction reactions. Such a complexation of reduced Ag nanoparticles with a polyelectrolyte multilayer matrix causes significant stress accumulation that then results in surface wrinkling. While conventional wrinkling systems can be characterized by discrete layers of different mechanical properties of the films, the PEM wrinkling of interest here deals with a nondiscrete single layer, wherein the degree of complexation of Ag into a swollen PEM film varies with the diffusion depth of the cationic exchange reaction, which is accompanied by a gradational change in mechanical properties. Therefore, a different approach that can be discerned from conventional theoretical analysis is required.

In addition, when the plasma-ashing process is applied to the polyelectrolyte/Ag complexed surface and the polymeric matrix is selectively removed, it can be expected that the hierarchically textured Ag nanostructures will remain on the surface. Since Ag nanostructures are sequentially reduced from the top surface of the polyelectrolyte multilayer matrix penetrating down into the inner film along the direction of cationic diffusion, structures of wedge-like nanoplates or nanoflakes are formed with a hierarchical order. Therefore, after the surface is chemically modified with a fluorinated species, the resulting surface shows superhydrophobic characteristics, on which the water contact angle reaches 170° and the sliding angle is less than 1°. The proposed nanostructuring method based on the spontaneous surface wrinkling can provide large-scale production capability, as well as tunability over structural characteristics; thus, a variety of applications are possible, such as functional coatings, optical films, and microfluidic devices.

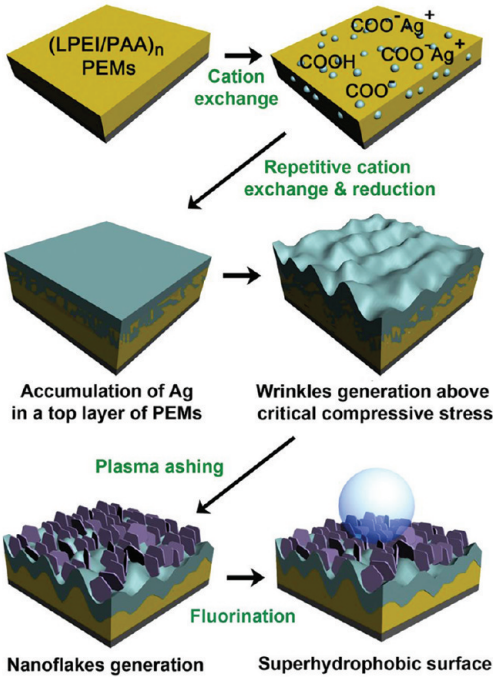


**Figure 1. Schematic illustration of the generation of the hierarchical nanoflake structure of Ag using surface wrinkling of polyelectrolyte/Ag complexed thin films. Sequential procedures consist of polyelectrolyte multilayer film deposition, cationic exchange and Ag reduction, surface wrinkling, plasma ashing for nanostructuring, and superhydrophobic surface modification.**

## RESULTS AND DISCUSSION

Figure 1 shows a procedure to fabricate hierarchical nanoflake structures by inducing the surface wrinkling of a polyelectrolyte/Ag composite, followed by plasma ashing of the polymeric matrix. In this study, we used a polyelectrolyte pair of linear polyethylenimine (LPEI) and poly(acrylic acid) (PAA), in which the notable interdiffusion characteristics and complementarily modified internal binding of polyelectrolyte chains facilitate the incorporation process with metallic Ag species.[23,24] Since the nontreated LPEI/PAA multilayer film is susceptible to dissociation caused by Ag ion impregnation, the LPEI/PAA multilayer film is cross-linked overnight with 1-ethyl-3-(3-dimethylaminopropyl) carbodiimide hydrochloride (EDC) treatment to strengthen the mechanical stability of the film.[25,26] In the experiment, the surface of the polyelectrolyte multilayered film is first treated with a deposition of negatively charged PAA to allow for the impregnation of positively charged Ag ions into the inner film. This cationic exchange reaction occurs when LPEI/PAA multilayered film is immersed in the silver acetate

solution, wherein the carboxyl groups in PAA strongly attract Ag ions.[27] The accumulated Ag ions are then reduced to Ag metal nanoparticles with a dimethylaminoborane (DMAB) reducing agent. Since the concentration of Ag ions is higher in the surface region, a relatively rigid polyelectrolyte/Ag composite layer is formed on the film surface after the Ag reduction process.

When the procedure of cationic exchange and subsequent reduction is repeatedly applied to the film, the Ag content in the surface region gradually increases, which brings about stress accumulation due to volume expansion. However, since the polyelectrolyte/Ag composite film is strongly adhered to the substrate, the volumetric expansion generates a lateral compressive stress, thereby leading to surface wrinkling with wavelength ranges on the order of micrometers. A plasma-ashing process is then applied to the polyelectrolyte/Ag composite film for selective removal of the polymeric phase. The resulting Ag structures exhibit plate-like or flake-like morphological characteristics with sizes ranging from several tens to hundreds of nanometers. Therefore, a hierarchically ordered nanoflake structure is generated on the surface in a combination with micrometer-scale wrinkles. Although the plasma-treated surface generally shows hydrophilic characteristics due to an excessive generation of hydroxyl groups, the nanoflake structure can be readily modified to a hydrophobic surface after treatment with fluorinated chemicals.[28] Therefore, one can expect to obtain superhydrophobicity based on the hierarchically developed surface structures.

Structural characteristics of the hierarchical nanoflake structure can be preemptively controlled by the size of the surface wrinkles. As has been generally confirmed in conventional wrinkling studies, a variation in the film thickness is mainly responsible for the size of the wrinkling wavelength.[29−31] Figure 2 shows a tendency of the wavelength change in response to the number of polyelectrolyte depositions. Two-dimensional atomic force microscopic (AFM) images show a monotonic increase in the characteristic wrinkling wavelength in accordance with an increase in the film thickness. The randomness of surface wrinkles can be verified by isotropic ring patterns manifested in the fast Fourier transform (FFT) analysis. Also, a decrease in the ring diameter of FFTs indicates gradual growth in the wrinkling wavelength. In experiments, the onset of surface wrinkling has been specifically observed at three time repetitions of cationic exchange and subsequent reduction, at which point the critical wrinkling stress was reached. When the film thickness is thin (8 bilayer depositions), the system requires a greater critical stress for wrinkling.[32] Therefore, a relatively small amount of residual stress that is exempt from the critical wrinkling stress is available for surface wrinkling, which renders morphologically spinodal-like

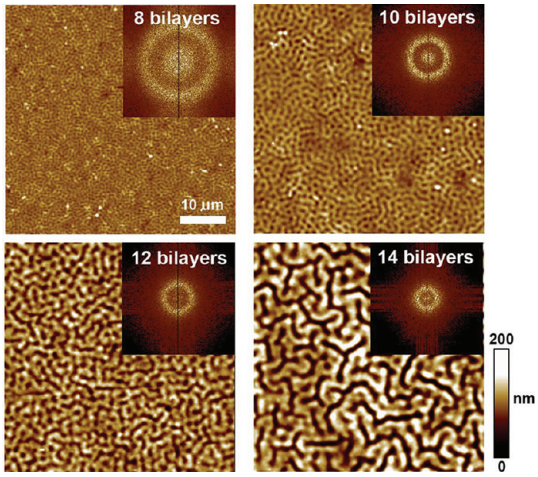


**Figure 2. Effect of film thickness (number of polyelectrolyte multilayer deposition) on the resulting wrinkling wavelength. Two-dimensional AFM images of surface wrinkles (50 $\mu$m $\times$ 50 $\mu$m, *z*-scale is 200 nm) with varying LbL deposition number of LPEI/PAA multilayers. The insets (FFT) reveal a gradual increase in wrinkling wavelength. The corresponding characteristic wrinkling wavelengths are 0.84 $\mu$m for 8 bilayers, 1.56 $\mu$m for 10 bilayers, 1.95 $\mu$m for 12 bilayers, and 2.80 $\mu$m for 14 bilayers.**

small wrinkles that correspond to an early stage of the wrinkling. On the other hand, when the film is thick (more than 12 bilayer depositions), a relatively large amount of residual stress can allow for wrinkling, leading to formation of well-developed surface wrinkles with labyrinthine structures.

Notably, the inner structure of the polyelectrolyte/Ag composite film used in this study cannot be characterized with discrete layers like those in conventional wrinkling systems. Rather, since the fractional composition of Ag in the film gradationally varies, a nondiscrete and indistinguishable interface is considered, as shown in the schematic in Figure 3A. In order to verify the gradationally varying distribution of Ag, we observed evolutionary changes in the film cross sections in response to an increase in the number of Ag reduction cycles. As revealed in serial scanning electron micrographs shown in Figure 3B, an initial film with a thickness of 320 nm (11 bilayers of LPEI/PAA) gradually grew to 450 and 650 nm when increasing the Ag reduction number to three and five cycles, respectively, which is indicative of volumetric expansion due to the incorporation of reduced Ag. Also, the observation of cross sections illustrates the formation of an indistinguishable interface between the top and bottom regions of the film, as well as the growth of surface wrinkles. Therefore, the conventional understanding of the wrinkled system as being separately composed of a rigid capping layer and a soft underlying layer cannot be applied to this system; in turn, traditional linear stability analysis cannot be directly employed for theoretical interpretation.[33−35] In order to elaborate on this specific wrinkling case, we investigate a wrinkling

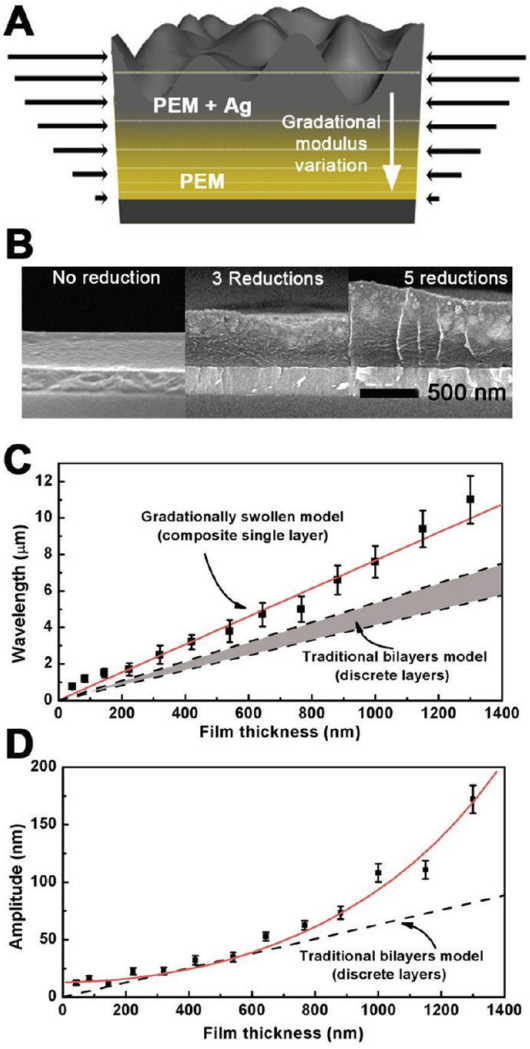


**Figure 3. Wrinkling instability analysis based on the gradationally swollen film model. (A) Schematic of the gradationally varying modulus in the polyelectrolyte/Ag complexed films. Due to the incorporation of reduced Ag, volumetric expansion is amplified along the axial direction and reaches the maximum at the surface. (B) Cross-sectional SEM observation for the volumetric expansion of the polyelectrolyte/Ag complexed films. Initially, 11 bilayered film of LPEI/PAA is swollen and expanded with increasing Ag reduction number. (C) Plot of characteristic wrinkling wavelength with respect to film thickness of LPEI/PAA polyelectrolyte multilayers after three cycles of Ag reduction. A solid red line is added to clarify the effectiveness of the gradationally swollen film model for this system. Error bars indicate the standard deviation. The gray-shaded region accounts for the estimated wavelength values based on the traditional bilayer wrinkling model. The upper dashed line corresponds to a pure Ag top layer ($E_m \sim 83$ GPa), and the lower one corresponds to a complexed Ag top layer ($E_m \sim 17.2$ GPa). (D) Plot of wrinkling amplitude with respect to film thickness of LPEI/PAA polyelectrolyte multilayers. The dotted line represents the estimated wrinkling amplitude based on the traditional bilayer wrinkling model, and the solid red line is the best fit of the measured amplitudes. Error bars indicate the standard deviation.**

model for a gradationally swollen system wherein the mechanical properties of the films vary vertically in response to the degree of film swelling.[36] Our system is substantially analogous to the case of swollen film wrinkling because the mechanical properties of the polyelectrolyte/Ag composite films can be manipulated by the interpenetration depth of Ag ions during the cationic exchange reaction. Therefore, after a reduction to Ag nanoparticles, a compositional change according to the degree of Ag incorporation follows the Ag ion concentration that varies gradationally within the films. In addition, similar to the swelling-induced osmotic pressure that drives wrinkling in the swollen film model, the nanoparticle-incorporation-induced pressure brings about surface wrinkling in this system. Therefore, on the basis of the model of surface waves with vertical stretching, wrinkling instability in the swollen films can be associated with the compressive surface pressure ($p$) as follows:[36,37]

$$p = \left(E_t^{1/2}\frac{kh}{3} - E_b^{1/2}\frac{1}{kh}\right)^2 + \frac{2}{3}(E_tE_b)^{1/2} \qquad (1)$$

Also, the critical surface pressure ($p_c$) and corresponding wrinkling wavelength ($\lambda_c$) for the first mode wrinkling instability can be expressed as

$$p_c = \frac{2}{3}(E_tE_b)^{1/2},\ k_c = \frac{2\pi}{\lambda_c} = \left(\frac{E_b}{E_t}\right)^{1/4}\frac{\sqrt{3}}{h} \qquad (2)$$

where $E$ is Young's modulus, $k$ is the wavenumber, $\lambda$ is the characteristic wrinkling wavelength, and $h$ is the film thickness. The subscripts "t" and "b" represent the top surface region and the near-substrate region, respectively. As shown in Figure 3C, theoretically estimated characteristics of the wrinkling wavelength based on a model of the swollen film instability agree well with the experimental results. However, the traditional model of bilayer wrinkling (gray shaped region in Figure 3C) shows the underestimated wave-growth characteristics compared to those from the gradationally swollen film model.[38]

While the modulus of the surface region in the gradationally swollen film model is much smaller than that of the bottom region due to the aqueously swollen environment,[36] in this system, the Young's modulus of the upper region in the polyelectrolyte/Ag composite film is greater than that of the lower region. In addition, while the swollen film model deals with mechanically soft characteristics, the chemically cross-linked matrix of the LPEI/PAA multilayer film exhibits relatively rigid characteristics. However, in spite of this contrasting nature, the onset of both cases can be attributed to the same instability condition in which the accumulated stress or compressive surface pressure is dissipated through bending deformation of the system by creating sinusoidal surface waves. In the case of swelling-induced osmotic pressure, the surface layer of gels is aqueously swollen and softened (softening due to the inclusion of low-modulus water), leading to volumetric expansion of the surface and subsequent wrinkling.

In parallel, for a system governed by nanoparticle-incorporation-induced pressure, polyelectrolyte films are subject to complexation and are hardened with the incorporation of Ag nanoparticles (hardening due to the complexation with high-modulus Ag), which yields volumetric expansion of the surface and subsequent wrinkling.

Another advantage of employing the gradationally swollen film model for wrinkling analysis is that the mechanical properties of the polyelectrolyte/Ag composite film can be estimated by eq 2. According to the best fit result obtained from Figure 3C, the modulus ratio between the upper rigid and lower soft regions of the complexed film is found to be approximately 20, for which the theoretical model well matches the experimental results. Since the upper region is the complexed phase between cross-linked polyelectrolyte chains and reduced Ag, it is difficult to estimate the corresponding Young's modulus therein. On the other hand, the lower region near the substrate rarely includes Ag nanoparticles; thus, the local elastic property is mainly governed by the mechanical modulus of the polyelectrolyte multilayers. The Young's modulus of the polyelectrolyte multilayers can be estimated by means of "strain induced elastic buckling instability for mechanical measurements" (SIEBIMM).[20,39,40] For this, an LPEI/PAA multilayer-deposited polydimethylsiloxane (PDMS) substrate is subjected to an external compressive strain to generate surface wrinkles, from which the elastic modulus of the LPEI/PAA complexed thin film can be estimated (Supporting Information 1). Measurements are conducted in an aqueous environment to reflect the swollen condition of the complexed films. As a result, a relatively large Young's modulus of 860 MPa is obtained for the swollen LPEI/PAA multilayered film, which can be attributed to the chemical cross-linking effect in the film having undergone EDC treatment. Therefore, the expected 20-fold difference indicates that the effective Young's modulus of the upper complexed surface reaches 17.2 GPa, which seems reasonable considering the complexed condition between the polyelectrolyte multilayer matrix and Ag nanoparticles. The validity of applying the gradationally swollen film model can be better understood from the comparative studies presented in the Supporting Information 2.

Surface instability analysis for a system with gradationally varying mechanical properties was also investigated with a bifurcation analysis and corresponding numerical calculation.[41] Such an approach deals with a model system wherein plasma-induced oxidation and wrinkling occur on a thick PDMS substrate by means of oxygen diffusion, creating the graded mechanical properties in the surface region. This gradational change has been considered to have a diffusion profile either with an exponential or error function, which strongly differs from the conventional system with nongraded homogeneous films. We also took estimations from the bifurcation analysis to obtain the modulus ratio between the upper rigid and lower soft regions, resulting in a similar value to that from the previously used swollen film model; the modulus ratio was in the range between 20 and 35 (Supporting Information 3). However, since this approach is assumed to have an infinite substrate thickness (substrate thickness $\gg$ wrinkling wavelength), the swollen film model employed in this study is believed to be more appropriate for analysis. Nevertheless, it is important to note that theoretical models that deal with the graded mechanical properties can well explain the wrinkling behaviors in experiments. In particular, they can propose a reasonable value for the estimation of the modulus ratio ($E_t/E_b \sim 20$), whereas it is highly overestimated for conventional approaches considering discrete layers (Supporting Information 2).

Along with the correlation between film thickness and the resulting wrinkling wavelength, we investigated the amplitude growth characteristics with respect to film thickness. Since the appropriate amplitude formula is not available for the gradationally swollen film model, the equilibrium amplitude adopted from a bilayer wrinkling model is considered as follows:[33]

$$A_{eq} = h_t\sqrt{\frac{1}{2}\left(\frac{N}{N_c} - 1\right)} \qquad (3)$$

where $N$ and $N_c$ are the membrane force and critical membrane force for wrinkling, respectively, and $h_t$ is the thickness of the top layer. In this system, wrinkling occurs spontaneously when the applied compressive stress exceeds the critical wrinkling stress, thus, we assume that the ratio of $N$ to $N_c$ is equal to 1.05, which agrees with the amplitude growth characteristic for the region of relatively thin films. However, as shown in Figure 3D, the estimated amplitude deviates severely from experiments as the thickness of the underlying polyelectrolyte multilayer increases. This change is possibly due to the fact that the wave amplification becomes prominent along the axial direction with film thickening. Since the volume expansion by the nanoparticle-incorporation-induced pressure is maximized at the surface (Figure 3A), the undulation by surface wrinkling is accordingly maximized and amplified, resulting in a nonlinearly increasing behavior in the wrinkling amplitude with increasing film thickness.

With a comprehensive understanding of estimated mechanical properties for the complexed film, the degree of complexation of Ag can be inferred by means of the modified Halpin–Tsai model.[42–44] This relationship is useful for estimating the elastic modulus of the composite materials, in which filler species are

incorporated into a matrix material.

$$\frac{E_{comp}}{E_m} = \frac{1+\xi\eta\phi}{1-\varphi\eta\phi}, \quad \xi \cong \frac{7-5\nu_m}{8-10\nu_m}, \quad \eta = \frac{(E_f/E_m)-1}{(E_f/E_m)+\xi}$$

$$\varphi = 1+\phi[(1-\phi_m)/\phi_m^2] \qquad (4)$$

where $E_{comp}$, $E_f$, and $E_m$ represent the Young's moduli of the composite, filler, and polymer matrix, respectively; $\nu_m$ is Poisson's ratio, $\xi$ is the shape parameter, $\eta$ is the Halpin–Tsai parameter that reflects the modulus ratio between the filler and matrix, $\phi$ is the volume fraction of filler, and $\phi_m$ is the maximum volumetric packing fraction. Therefore, in order to estimate the compositional fraction of Ag based on the Halpin–Tsai equation, we use 860 MPa as the Young's modulus of the cross-linked LPEI/PAA multilayers under aqueous condition, 83 GPa for that of the Ag nanoparticles, 0.5 for Poisson's ratio of swollen polymer matrix, and 0.64 for the maximum volumetric packing fraction on the basis of the random close packing condition of Ag nanoparticles.[45] Finally, taking into account the fact that the modulus ratio ($E_{comp}/E_m$) of 20 was obtained from the swollen film instability model, we estimate the Ag composition at the surface region of the complexed film as approximately 61%.

In order to compare the estimated Ag composition with the actual value, we employed characterization with energy-dispersive X-ray spectroscopy (EDX). As shown in Figure 4, an initially 400 nm thick LPEI/PAA film is expanded to 550 nm after three repetitive cycles of the Ag reduction process. From EDX characterization results, major elemental peaks are C, O, and Ag, among which C and O species are treated to be originated from polymeric matrix. After a conversion of the elemental weight fraction into a volume fraction,[27] as a result, EDX measurements reveal that the volumetric content of Ag in the surface layer reaches the maximum of 34.7%, then gradually decreases to 14.2% near the substrate. While the gradationally varying tendency of the incorporated Ag composition is verified with EDX measurements, the obtained results show a relatively large difference compared to the estimated values. This difference can be ascribed to the fact that the directional diffusion-induced, interconnected structures of Ag significantly reinforce the mechanical property of the composite film. On the other hand, the Halpin–Tsai complexation model is based on the simple mixing of individual spherical particles in the matrix without the formation of interconnected structures, which alleviates the influence of complexation on mechanical hardening.[42]

Figure 5A shows the evolutional growth of wrinkles as the number of Ag reductions increases with a fixed polyelectrolyte multilayer film thickness. First observed wrinkles at three time reductions gradually grow to well-developed labyrinthine structures after applying seven time reductions. Notably, in spite of the continuous growth of wrinkles, the characteristic wrinkling

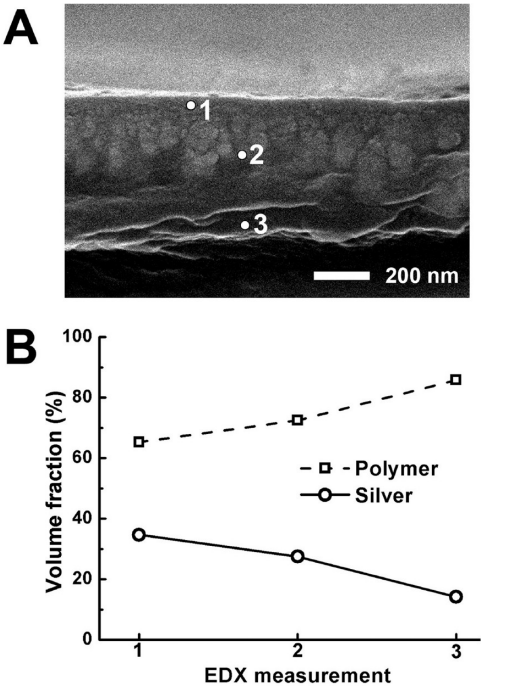


**Figure 4. Energy-dispersive X-ray spectroscopic (EDX) characterization of the polyelectrolyte/Ag complexed films. (A) Cross-sectional SEM observation for EDX measurements. The cross section shows a gradational distribution and complexation of Ag within the matrix of polyelectrolyte multilayer film. (B) Variation of the relative volumetric composition of the polyelectrolyte/Ag complexed films. The Ag content gradually decreases from the top surface region to the bottom region near the substrate.**

wavelength is observed to be constant. This can be attributed to the stepwise growth characteristics of the elastically induced wrinkling systems.[46] When the critical wrinkling stress is exceeded, the characteristic wrinkling wavelength can be determined by the instability condition of the system. After the initial formation of wrinkles on the surface, additionally applied strain is consumed by amplifying the wrinkles while maintaining the wavelength. However, if the reduction process is repeatedly applied to reach the saturation limit of wave amplification, then, a transition from wrinkling to delamination takes place, whereby the accumulated stress is instantaneously released.[47] As shown in the AFM image in Figure 5B, the surface topology after delamination shows tens of micrometer-scale undulations and the disappearance of intrinsically formed wrinkles. The delaminated film structure is proved by cross-sectional observation with the scanning electron microscope (SEM), manifesting complete detachment of the film from the substrate and a formation of the separate interface after a larger number of Ag reductions.

As confirmed from the SEM observational results, the wrinkled surface has a hierarchical structure on which Ag nanobumps of several tens of nanometers are embedded within the wrinkles with micrometer-sized wavelengths. Also, the results from the previous theoretical estimation and EDX measurements suggest

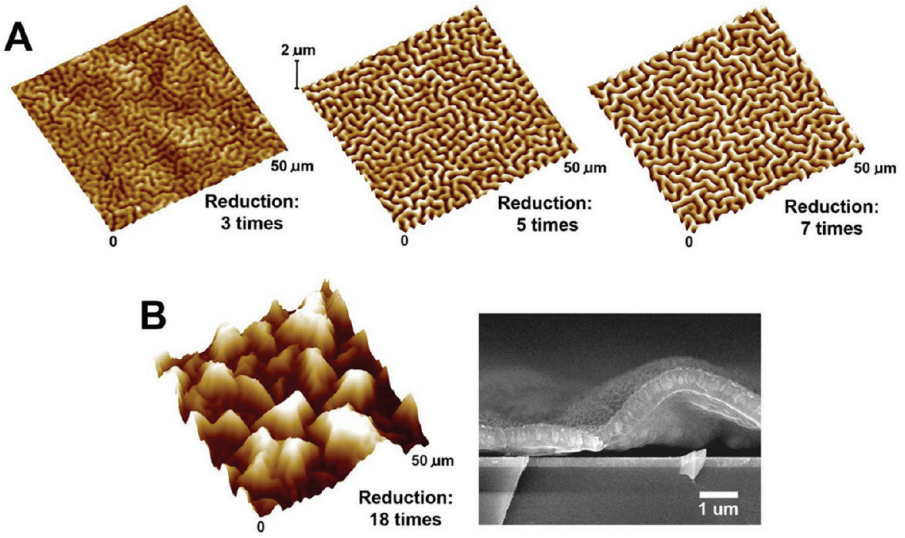


**Figure 5. Effect of reduction number of Ag on the morphology of surface wrinkles. The initial film thickness is fixed at 420 nm (13 bilayers of LPEI/PAA). (A) Three-dimensional AFM images of surface wrinkles (50 $\mu$m $\times$ 50 $\mu$m, *z*-scale is 2 $\mu$m) with varying the reduction number of Ag. The amplitude of wrinkles gradually increases while maintaining a constant wavelength (from three to seven cycles of reduction). (B) Three-dimensional AFM and cross-sectional SEM images of delaminated wrinkles. Delamination occurs after excessive reduction of 18 cycles.**

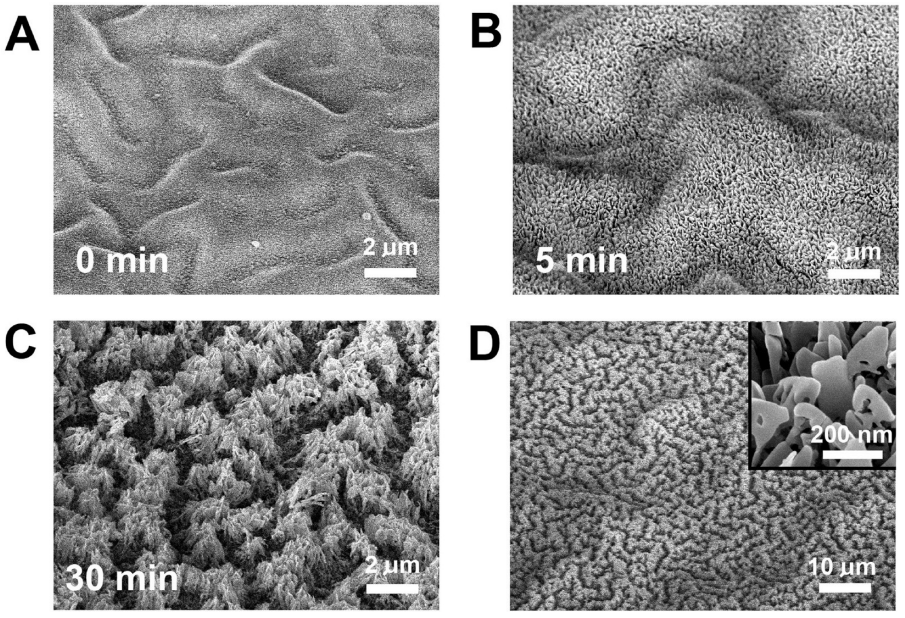


**Figure 6. Hierarchical nanoflake structure of Ag and its superhydrophobic surface characteristic. (A–C) SEM images of the evolution of surface texture with varying plasma-ashing time. An initial wrinkled surface (A, 0 min) is roughened with nanoscale Ag flakes (B, 5 min), and further developed to hierarchical nanoflake wrinkles (C, 30 min). (D) Low-magnification SEM image for C. Intrinsically formed microscale wrinkles are clearly manifested. The inset shows a highly magnified image of the vertical Ag nanoflake structure.**

that the degree of complexation of Ag nanoparticles inside the film gradually decreases from the maximum at the top to the minimum near the substrate. Therefore, with the aid of an appropriate plasma-ashing process, the metallic Ag nanostructures on the surface can be exposed by selectively removing the polymeric matrix. This kind of hierarchical structure can exhibit superhydrophobic surface characteristics.[48–50] Although superhydrophobic surfaces fabricated by structural engineering of polyelectrolyte multilayer films have been previously investigated,[51,52] the means proposed in this study offer a greater opportunity to elaborately manipulate the topological characteristics of hierarchical structures. Figure 6 shows the results of time-evolutional change in surface structures for an increased duration of plasma ashing. Although the initial surface (Figure 6A) shows a structural hierarchy, it cannot achieve complete superhydrophobicity due

primarily to a low aspect ratio structure of Ag nanobumps. Meanwhile, if the plasma-ashing process is applied for 5 min (Figure 6B) or 30 min (Figure 6C), the polymeric matrix around the Ag nanobumps is selectively removed, leaving a nanoflake-shaped and high aspect ratio Ag surface. Since the Ag nanoflakes are aligned along the initially developed surface wrinkles, the hierarchical characteristic of the system is reinforced (Figure 6D). In particular, an advantage of the spontaneous and parallel processing of this method is capable of implementing large area fabrication of structured surfaces (2 in. × 6 in., Supporting Information 4).

As can be verified from the inset in Figure 6D, the vertical nanoflake structure can offer better tunability with regard to the orientation and exquisiteness of the structures than other petal-like or flake structures prepared by chemical deposition or electrochemical reaction methods.[53−56] Previous approaches have mainly utilized a solution-based environment such that generated structures could have a high degree of isotropy during structure generation. In contrast, the method presented here takes advantage of the directional diffusion of Ag ions and the subsequent reduction within polyelectrolyte complex films, eventually inducing the formation of a highly vertical and anisotropically aligned nanoflake structure with a high aspect ratio. Although the freshly prepared hierarchical nanoflake structure shows a hydrophilic surface property due to the excessive generation of surface hydroxyl groups during exposure to the plasma-ashing process, it can be readily modified to a superhydrophobic surface by treatment with fluorinated self-assembled monolayer materials, such as 1*H*,1*H*,2*H*,2*H*-perfluorooctyltriethoxysilane.[57] After the surface is chemically modified, as shown in Figure 7A, the water contact angle is 170°, and the sliding angle of water drop is less than 1°, representing the superhydrophobic surface characteristics. Such a superhydrophobicity is amenable to a typical case of Cassie contact, wherein numerous nanoscale voids within the hierarchical structures spontaneously repel water drops and prevent surface wetting.[58,59] In order to verify the structural efficacy of the hierarchical nanoflake structure to the superhydrophobic surface property, we tested the water contact angles of the nanoflake surface according to the structural variation by controlling the plasma-ashing time (Figure 7B). When the nanoflake structure is developed in the absence of the hierarchical wrinkles, moderate hydrophobicity with a contact angle hysteresis is observed (first group, no wrinkles), which underpins the importance of the hierarchically formed wrinkles for obtaining the superhydrophobicity.[60] On the other hand, when the surface is only covered with microscale wrinkles embedded with Ag nanobumps, the surface shows mitigated hydrophobicity with a larger contact angle hysteresis (second group, no ashing treatment). However, as the

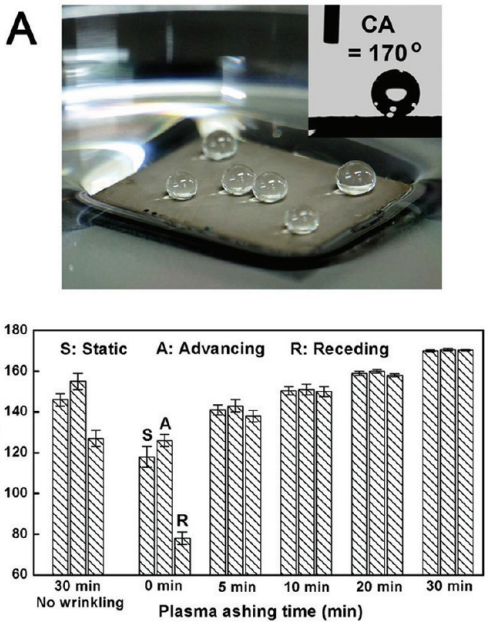


**Figure 7. (A) Superhydrophobic property of the surface of the hierarchical nanoflake structure. The water contact angle is 170°, and the sliding angle is less than 1°. The snapshot shows that small water drops are stably placed on the structured sample that is floating on the water surface (an ideally horizontal surface). (B) Measurements of dynamic contact angle of water droplets on differently treated nanoflake surfaces with varying plasma-ashing time. The hysteresis between advancing and receding contact angles is observed for wrinkle-free or nanoflake-free surfaces.**

plasma-ashing time increases, the synergistic effect of the combination of Ag nanoflakes and underlying microwrinkles becomes more prominent, eventually leading to the superhydrophobicity of 170° with no contact angle hysteresis.

Finally, in order to prove the usefulness of the hierarchical nanoflake structure based on the LPEI/PAA multilayer matrix, we replaced the polyelectrolytes pair with poly(allylamine hydrochloride) (PAH) and PAA, which is a typical pair of weakly charged polyelectrolytes.[61,62] Here, PAH/PAA multilayer film was assembled at a low pH condition of 2.5. Although the spontaneous interdiffusion of polyelectrolyte chains is not allowed for this system, the interpenetration of metal ions into the PAH/PAA complexed matrix during the cationic exchange reaction is highly facilitated due to a high density of free acid groups in PAA under acidic conditions. To compare the characteristics of nanoparticle incorporation and the resulting deformation of the surface, 18 bilayers of LPEI/PAA and 40 bilayers of PAH/PAA multilayered films were prepared and then subsequently treated with 9 cycles of Ag reduction. As contrasted in the cross-sectional SEM images in Figure 8, two systems showed completely different behaviors in sequestering Ag ions. While the gradationally complexed Ag distribution and localized volume expansion at the surface region were observed for LPEI/PAA multilayer films (Figure 8A), a uniform

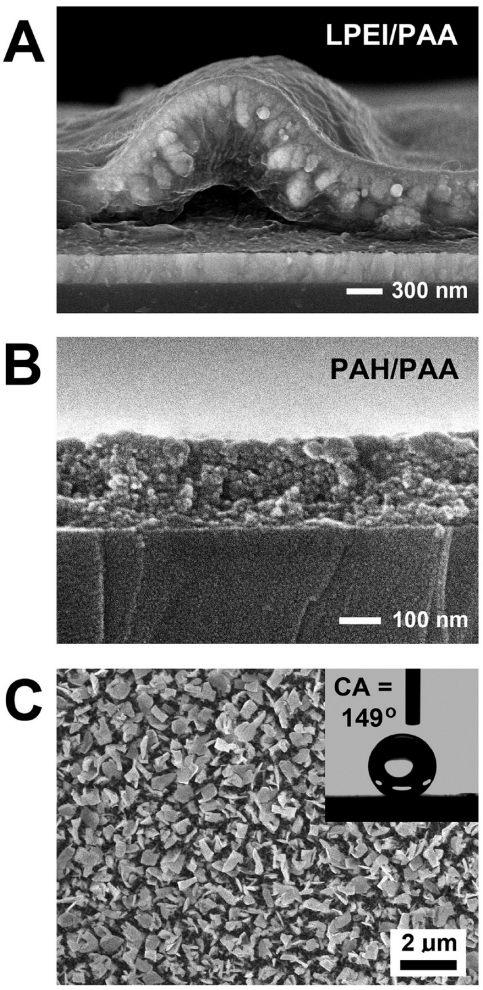


**Figure 8. Comparison of the cross section for different types of Ag complexed polyelectrolyte multilayered films. (A) Eighteen bilayers of LPEI/PAA film complexed with Ag by nine cycles of Ag reductions. (B) Forty bilayers of PAH/PAA film complexed with Ag by nine cycles of Ag reductions. (C) SEM image of structured Ag surface after 30 min of plasma ashing based on the PAH/PAA multilayer matrix.**

distribution of Ag nanoparticles and slight surface roughening were captured in the PAH/PAA multilayer films (Figure 8B). In particular, for a PAH/PAA system, nanoparticles approximately 10−15 nm in diameter completely fill the polymeric matrix, manifesting an outstanding capability as a nanochemical reactor for particle synthesis. However, due to this high uniformity in particle distribution, the PAH/PAA system is not amenable to film instability or surface wrinkling.

This difference in the Ag particle distribution can be ascribed to the binding strength of the ionic complexes assembled with oppositely charged polyelectrolyte chains. When nontreated LPEI/PAA complexed films are subject to cationic exchange reaction, films are readily dissociated due to the weakly bound characteristics between LPEI and PAA. After being chemically cross-linked with EDC, the LPEI/PAA multilayered films can be mechanically strengthened to allow for cationic exchange and Ag reduction reactions. However, due to the presence of the permanently cross-linked networks inside the films, the incorporation process of Ag nanoparticles is spatially limited near the surface region and leads to the graded distribution, further leading to a formation of surface wrinkles. On the other hand, PAH/PAA multilayered films have an intrinsically stronger internal binding than that of the LPEI/PAA pair, thus, cationic exchange reaction and subsequent Ag reduction process can successfully occur inside the polymeric matrix without sacrificing the mobility of Ag ions, rendering a uniform distribution of Ag nanoparticles. Since the preferential accumulation of the mechanical stress in the film has not occurred, no wrinkles are formed on the surface. When PAH/PAA films are treated with EDC for a chemical cross-linking, however, the cross-linked networks are rarely developed due to the deficiency in ionic bonding between charged carboxylate and ammonium groups under the assembly pH condition of 2.5, yielding a similar behavior of Ag reduction to the non-cross-linking-treated PAH/PAA films. These results indicate a significant role of the binding strength between charged polyelectrolyte chains for creating the graded complexation behavior and subsequent occurrence of the surface wrinkling. Accordingly, we expect that different surface morphologies of Ag nanostructures can be obtained depending on the type of polyelectrolyte multilayer matrix. While a distinctive structural hierarchy is obtained for the case of the LPEI/PAA matrix (Figure 6A−D), a randomly scattered phase of Ag nanoflakes is observed for the case of the PAH/PAA matrix (Figure 8C). Since the structural hierarchy is deficient and the flake size is relatively larger than that from the LPEI/PAA pair, Ag nanostructures obtained from the PAH/PAA matrix show a smaller water contact angle of 149° after the chemical modification of the surface.

## CONCLUSION

In summary, a novel and robust approach to produce a hierarchical nanoflake surface is obtained by controlling the wrinkling phenomena on a thin film that is complexed between polyelectrolyte multilayers and metallic Ag nanoparticles. The resulting surface structures exhibit a well-defined hierarchy, wherein the vertically aligned Ag nanoflakes are densely embedded within the micrometer-scale surface wrinkles. This structural hierarchy is capable of creating superhydrophobic surface characteristics (water contact angle = 170°) over a large area. In order to obtain structural tunability for the system, we take into account elaborate control over the size of surface wrinkles and the aspect ratio of the nanoflake structure, for which the degree of complexation of nanoparticles and the pair of polyelectrolyte multilayers are varied. In addition, to obtain a more quantitative understanding of the wrinkling of complexed thin films, a wrinkling instability analysis based

on the gradationally swollen film model is employed, such that the theoretical estimation well matches the experimental results. Moreover, this theoretical analysis enables the precise estimation of the mechanical modulus of complexed thin films. Therefore, we envision that this method will be applied to industrial-scale surface structuring, surface modification in microfluidic devices, or noble textures for optical devices.

## METHODS

**Preparation of Layer-by-Layer (LbL) Assembly of Polyelectrolyte Multilayers.** Linear polyethylenimine (LPEI, 25 000 $M_w$) and poly(acrylic acid) (PAA, 90 000 $M_w$, 25% aqueous solution) were purchased from Polysciences. Poly(allylamine hydrochloride) (PAH, 56 000 $M_w$) was purchased from Aldrich. All chemicals were used as received. LPEI and PAA were prepared as 35 and 20 mM solutions in deionized water, respectively, based on the repeat-unit molecular weight. For a pair of PAH and PAA, solutions were prepared as 20 mM without salt dissolution. The pH values of the LPEI and PAA solutions were carefully adjusted to 4.7 with dilute solutions of hydrochloric acid and sodium hydroxide, and the pH values of the PAH and PAA solutions were adjusted to 2.5 and 2.5, respectively. A cleaned slide glass was used as a substrate for the LbL deposition. In order to provide hydrophilicity for the successful adsorption of polyelectrolytes in the aqueous condition, the glass substrate was slightly plasma-treated with a conventional plasma cleaner for 30 s (PDC-001, Harrick Scientific Corp.). Layer-by-layer deposition was performed using a programmable slide stainer (HMS70, Microm) under the deposition conditions of polyelectrolyte adsorption for 10 min followed by three sequential washing steps (1 min for each) in a deionized water bath.

**Fabrication of Wrinkled Surfaces.** Before applying the surface wrinkling process, LbL-deposited polyelectrolyte multilayer films were immersed in a 5 mM solution of 1-ethyl-3-(3-dimethylaminopropyl) carbodiimide hydrochloride (EDC, Thermo Scientific) and cross-linked overnight to increase the mechanical stability. The cross-linked films were then immersed in a 5 mM solution of silver acetate (Aldrich) for 10 min. This process facilitated a cationic exchange reaction so that Ag ions could strongly bind to carboxyl groups in polyelectrolyte chains of PAA. After thoroughly washing the samples with deionized water, samples were reacted with 1 mM aqueous solution of dimethylaminoborane (DMAB, Aldrich) for 10 min to induce the reduction of Ag ions captured within the films to Ag nanoparticles. This unit procedure was repeatedly applied to the samples using a programmable slide stainer until surface wrinkling occurred.

**Fabrication of Superhydrophobic Surfaces.** Samples of wrinkled polyelectrolyte/Ag complexed films were plasma-etched to selectively remove the polyelectrolyte multilayer matrix (plasma ashing). As a result, a hierarchically developed Ag nanoflake structure was formed on the surface. The aspect ratio of the nanoflake structure could be controlled by varying the plasma-ashing time. In order to generate a superhydrophobic surface characteristic, samples were then treated with 1*H*,1*H*,2*H*,2*H*-perfluorooctyltriethoxysilane (POTS, Aldrich, 1 wt % in methyl alcohol) for 1 h. Finally, the fluorinated surfaces were stabilized with a thermal annealing process at 140 °C for 2 h.

**Characterization of Hierarchical Nanoflake Structured Surface.** The thickness of the deposited polyelectrolyte multilayers was measured by ellipsometry (Nanoview, SEMF-1000, Korea). The changes in the surface topology of the wrinkled polyelectrolyte/Ag complexed thin films were observed with an atomic force microscope (AFM, Dimension 3100, Veeco, Plainview, NY) under dry condition. In order to minimize any possible errors during data acquisition and to enhance the image resolution, we used the tapping mode at a slow scanning rate (scan speed of 0.5−1.0 Hz). To visualize the surface textures and cross section of samples, we used scanning electron microscope (SEM, JSM-7401F, JEOL). The elemental analysis was performed with energy-dispersive X-ray spectroscopy (EDX, Oxford Instruments, INCA-PentaFET-x3 detector) that was attached to the SEM. Finally, to measure the static contact angle with sessile droplet mode, deionized water with a droplet volume of 5 $\mu$L was dispensed on the hierarchical nanoflake structure of polyelectrolyte/Ag complexed films. The contact angles were measured using contact angle goniometer (FM40, KRUSS, Germany) by averaging over five different points. In addition, using a handmade setup, the sliding angle was measured by tilting the substrate.

*Acknowledgment.* This work was supported by Basic Science Research Program grants (2010-0009877, 2010-0029409) and research grant (NRF-C1AAA001-2010-0028962) through the National Research Foundation of Korea (NRF) funded by the Korea Government (MEST). This work was also supported by National Platform Technology grant (10033871) under the Ministry of the Knowledge Economy of Korea. The authors also acknowledge the `Hi Seoul Science/Humanities Fellowship' from Seoul Scholarship Foundation.

*Supporting Information Available:* SIEBIMM characterization for LPEI/PAA multilayer films; theoretical comparison between the gradationally swollen film wrinkling model and the multilayer instability model; estimation of the modulus ratio using bifurcation analysis; video clip of large-scale demonstration of superhydrophobic surface. This material is available free of charge *via* the Internet at http://pubs.acs.org.

## REFERENCES AND NOTES

1. Xia, F.; Jiang, L. Bio-Inspired, Smart, Multiscale Interfacial Materials. *Adv. Mater.* **2008**, *20*, 2842–2858.
2. Sotiropoulou, S.; Sierra-Sastre, Y.; Mark, S. S.; Batt, C. A. Biotemplated Nanostructured Materials. *Chem. Mater.* **2008**, *20*, 821–834.
3. Jeong, H. E.; Lee, J. K.; Kim, H. N.; Moon, S. H.; Suh, K. Y. A Nontransferring Dry Adhesive with Hierarchical Polymer Nanohairs. *Proc. Natl. Acad. Sci. U.S.A.* **2009**, *106*, 5639–5644.
4. Qiu, J. H.; Guo, M.; Wang, X. D. Electrodeposition of Hierarchical ZnO Nanorod-Nanosheet Structures and Their Applications in Dye-Sensitized Solar Cells. *ACS Appl. Mater. Interfaces* **2011**, *3*, 2358–2367.
5. Rahmawan, Y.; Jang, K. J.; Moon, M. W.; Lee, K. R.; Suh, K. Y. Anti-Biofouling Coating by Wrinkled, Dual-Roughness Structures of Diamond-like Carbon (DLC). *Biochip J.* **2009**, *3*, 143–150.
6. Magasinski, A.; Dixon, P.; Hertzberg, B.; Kvit, A.; Ayala, J.; Yushin, G. High-Performance Lithium-Ion Anodes Using Hierarchical Bottom-Up Approach. *Nat. Mater.* **2010**, *9*, 353–358.
7. Zhang, H.; Cao, G. P.; Wang, Z. Y.; Yang, Y. S.; Shi, Z. J.; Gu, Z. N. Growth of Manganese Oxide Nanoflowers on Vertically-Aligned Carbon Nanotube Arrays for High-Rate Electrochemical Capacitive Energy Storage. *Nano Lett.* **2008**, *8*, 2664–2668.
8. Lee, Y. M.; Kim, Y. H.; Lee, J. H.; Park, J. H.; Park, N. G.; Choe, W. S.; Ko, M. J.; Yoo, P. J. Highly Interconnected Porous Electrodes for Dye-Sensitized Solar Cells Using Viruses as a Sacrificial Template. *Adv. Funct. Mater.* **2011**, *21*, 1160–1167.
9. Pokroy, B.; Kang, S. H.; Mahadevan, L.; Aizenberg, J. Self-Organization of a Mesoscale Bristle into Ordered, Hierarchical Helical Assemblies. *Science* **2009**, *323*, 237–240.
10. Ahn, D. U.; Wang, Z.; Yang, R. G.; Ding, Y. F. Hierarchical Polymer Patterns Driven by Capillary Instabilities at Mobile

and Corrugated Polymer-Polymer Interfaces. *Soft Matter* **2010**, *6*, 4900–4907.
11. Zhou, S. H.; Ma, Z.; Baker, G. A.; Rondinone, A. J.; Zhu, Q.; Luo, H. M.; Wu, Z. L.; Dai, S. Self-Assembly of Metal Oxide Nanoparticles into Hierarchically Patterned Porous Architectures Using Ionic Liquid/Oil Emulsions. *Langmuir* **2009**, *25*, 7229–7233.
12. Vandeparre, H.; Gabriele, S.; Brau, F.; Gay, C.; Parker, K. K.; Damman, P. Hierarchical Wrinkling Patterns. *Soft Matter* **2010**, *6*, 5751–5756.
13. Ahn, S. H.; Guo, L. J. Spontaneous Formation of Periodic Nanostructures by Localized Dynamic Wrinkling. *Nano Lett.* **2010**, *10*, 4228–4234.
14. Yoo, P. J.; Lee, H. H. Morphological Diagram for Metal/Polymer Bilayer Wrinkling: Influence of Thermomechanical Properties of Polymer Layer. *Macromolecules* **2005**, *38*, 2820–2831.
15. Park, J. Y.; Chae, H. Y.; Chung, C. H.; Sim, S. J.; Park, J.; Lee, H. H.; Yoo, P. J. Controlled Wavelength Reduction in Surface Wrinkling of Poly(dimethylsiloxane). *Soft Matter* **2010**, *6*, 677–684.
16. Decher, G. Fuzzy Nanoassemblies: Toward Layered Polymeric Multicomposites. *Science* **1997**, *277*, 1232–1237.
17. Hammond, P. T. Form and Function in Multilayer Assembly: New Applications at the Nanoscale. *Adv. Mater.* **2004**, *16*, 1271–1293.
18. Hendricks, T. R.; Lee, I. Wrinkle-Free Nanomechanical Film: Control and Prevention of Polymer Film Buckling. *Nano Lett.* **2007**, *7*, 372–379.
19. Hendricks, T. R.; Wang, W.; Lee, I. Buckling in Nanomechanical Films. *Soft Matter* **2010**, *6*, 3701–3706.
20. Stafford, C. M.; Harrison, C.; Beers, K. L.; Karim, A.; Amis, E. J.; Vanlandingham, M. R.; Kim, H. C.; Volksen, W.; Miller, R. D.; Simonyi, E. E. A Buckling-Based Metrology for Measuring the Elastic Moduli of Polymeric Thin Films. *Nat. Mater.* **2004**, *3*, 545–550.
21. Yoo, P. J.; Lee, H. H. Complex Pattern Formation by Adhesion-Controlled Anisotropic Wrinkling. *Langmuir* **2008**, *24*, 6897–6902.
22. Yoo, P. J. Fabrication of Complexly Patterned Wavy Structures Using Self-Organized Anisotropic Wrinkling. *Electron. Mater. Lett.* **2011**, *7*, 17–23.
23. Yoo, P. J.; Zacharia, N. S.; Doh, J.; Nam, K. T.; Belcher, A. M.; Hammond, P. T. Controlling Surface Mobility in Interdiffusing Polyelectrolyte Multilayers. *ACS Nano* **2008**, *2*, 561–571.
24. Yoo, P. J.; Nam, K. T.; Belcher, A. M.; Hammond, P. T. Solvent-Assisted Patterning of Polyelectrolyte Multilayers and Selective Deposition of Virus Assemblies. *Nano Lett.* **2008**, *8*, 1081–1089.
25. Yang, S. Y.; Lee, D.; Cohen, R. E.; Rubner, M. F. Bioinert Solution-Cross-Linked Hydrogen-Bonded Multilayers on Colloidal Particles. *Langmuir* **2004**, *20*, 5978–5981.
26. Schuetz, P.; Caruso, F. Copper-Assisted Weak Polyelectrolyte Multilayer Formation on Microspheres and Subsequent Film Crosslinking. *Adv. Funct. Mater.* **2003**, *13*, 929–937.
27. Wang, T. C.; Rubner, M. F.; Cohen, R. E. Polyelectrolyte Multilayer Nanoreactors for Preparing Silver Nanoparticle Composites: Controlling Metal Concentration and Nanoparticle Size. *Langmuir* **2002**, *18*, 3370–3375.
28. Hong, J.; Bae, W. K.; Lee, H.; Oh, S.; Char, K.; Caruso, F.; Cho, J. Tunable Superhydrophobic and Optical Properties of Colloidal Films Coated with Block-Copolymer-Micelles/Micelle-Multilayers. *Adv. Mater.* **2007**, *19*, 4364–4369.
29. Genzer, J.; Groenewold, J. Soft Matter with Hard Skin: From Skin Wrinkles to Templating and Material Characterization. *Soft Matter* **2006**, *2*, 310–323.
30. Yoo, P. J.; Suh, K. Y.; Park, S. Y.; Lee, H. H. Physical Self-Assembly of Microstructures by Anisotropic Buckling. *Adv. Mater.* **2002**, *14*, 1383–1387.
31. Guvendiren, M.; Yang, S.; Burdick, J. A. Swelling-Induced Surface Patterns in Hydrogels with Gradient Crosslinking Density. *Adv. Funct. Mater.* **2009**, *19*, 3038–3045.
32. Allen, H. G. *Analysis and Design of Structural Sandwich Panels*; Pergamon: New York, 1969.
33. Huang, Z. Y.; Hong, W.; Suo, Z. Nonlinear Analyses of Wrinkles in a Film Bonded to a Compliant Substrate. *J. Mech. Phys. Solids* **2005**, *53*, 2101–2118.
34. Huang, Z. Y.; Hong, W.; Suo, Z. Evolution of Wrinkles in Hard Films on Soft Substrates. *Phys. Rev. E* **2004**, *70*, 030601.
35. Im, S. H.; Huang, R. Evolution of Wrinkles in Elastic-Viscoelastic Bilayer Thin Films. *J. Appl. Mech. Tech. ASME* **2005**, *72*, 955–961.
36. Tanaka, T.; Sun, S. T.; Hirokawa, Y.; Katayama, S.; Kucera, J.; Hirose, Y.; Amiya, T. Mechanical Instability of Gels at the Phase Transition. *Nature* **1987**, *325*, 796–798.
37. Landau, L. D.; Lifshitz, E. M. *Theory of Elasticity*; Pergamon: New York, 1969.
38. Chan, E. P.; Kundu, S.; Lin, Q.; Stafford, C. M. Quantifying the Stress Relaxation Modulus of Polymer Thin Films *via* Thermal Wrinkling. *ACS Appl. Mater. Interfaces* **2011**, *3*, 331–338.
39. Nolte, A. J.; Rubner, M. F.; Cohen, R. E. Determining the Young's Modulus of Polyelectrolyte Multilayer Films *via* Stress-Induced Mechanical Buckling Instabilities. *Macromolecules* **2005**, *38*, 5367–5370.
40. Nolte, A. J.; Cohen, R. E.; Rubner, M. F. A Two-Plate Buckling Technique for Thin Film Modulus Measurements: Applications to Polyelectrolyte Multilayers. *Macromolecules* **2006**, *39*, 4841–4847.
41. Lee, D.; Triantafyllidis, N.; Barber, J. R.; Touless, M. D. Surface Instability of an Elastic Half Space with Material Properties Varying with Depth. *J. Mech. Phys. Solids* **2008**, *56*, 858–868.
42. Halpin, J. C.; Kardos, J. L. The Halpin–Tsai Equations: A Review. *Polym. Eng. Sci.* **1976**, *16*, 344–352.
43. Nielsen, L. E. Generalized Equation for the Elastic Moduli of Composite Materials. *J. Appl. Phys.* **1970**, *41*, 4626–4627.
44. Wu, Y. P.; Jia, Q. X.; Yu, D. S.; Zhang, L. Q. Modeling Young's Modulus of Rubber-Clay Nanocomposites Using Composite Theories. *Polym. Test.* **2004**, *23*, 903–909.
45. Lewis, T. B.; Nielsen, L. E. Dynamic Mechanical Properties of Particulate-Filled Composites. *J. Appl. Polym. Sci.* **1970**, *14*, 1449–1471.
46. Yoo, P. J.; Lee, H. H. Evolution of a Stress-Driven Pattern in Thin Bilayer Films: Spinodal Wrinkling. *Phys. Rev. Lett.* **2003**, *91*, 154502.
47. Mei, H. X.; Huang, R.; Chung, J. Y.; Stafford, C. M.; Yu, H. H. Buckling Modes of Elastic Thin Films on Elastic Substrates. *Appl. Phys. Lett.* **2007**, *90*, 151902.
48. Lee, Y. W.; Park, S. H.; Kim, K. B.; Lee, J. K. Fabrication of Hierarchical Structures on a Polymer Surface To Mimic Natural Superhydrophobic Surfaces. *Adv. Mater.* **2007**, *19*, 2330–2335.
49. Rahmawan, Y.; Moon, M. W.; Kim, K. S.; Lee, K. R.; Suh, K. Y. Wrinkled, Dual-Scale Structures of Diamond-like Carbon (DLC) for Superhydrophobicity. *Langmuir* **2010**, *26*, 484–491.
50. Zhao, N.; Xu, J.; Xie, Q. D.; Weng, L. H.; Guo, X. L.; Zhang, X. L.; Shi, L. H. Fabrication of Biomimetic Superhydrophobic Coating with a Micro-Nano-Binary Structure. *Macromol. Rapid Commun.* **2005**, *26*, 1075–1080.
51. Zhai, L.; Cebeci, F. C.; Cohen, R. E.; Rubner, M. F. Stable Superhydrophobic Coatings from Polyelectrolyte Multilayers. *Nano Lett.* **2004**, *4*, 1349–1353.
52. Zhai, L.; Berg, M. C.; Cebeci, F. C.; Kim, Y.; Milwid, J. M.; Rubner, M. F.; Cohen, R. E. Patterned Superhydrophobic Surfaces: Toward a Synthetic Mimic of the Namib Desert Beetle. *Nano Lett.* **2006**, *6*, 1213–1217.
53. Liu, J. P.; Huang, X. T.; Li, Y. Y.; Li, Z. K.; Chi, Q. B.; Li, G. Y. Formation of Hierarchical CuO Microcabbages as Stable Bionic Superhydrophobic Materials *via* a Room-Temperature Solution-Immersion Process. *Solid State Sci.* **2008**, *10*, 1568–1576.
54. Cao, Z. W.; Xiao, D. B.; Kang, L. T.; Wang, Z. L.; Zhang, S. X.; Ma, Y.; Fu, H. B.; Yao, J. N. Superhydrophobic Pure Silver Surface with Flower-like Structures by a Facile Galvanic Exchange Reaction with $[Ag(NH_3)_2]OH$. *Chem. Commun.* **2008**, 2692–2694.
55. Liu, X. M.; He, J. H. One-Step Hydrothermal Creation of Hierarchical Microstructures toward Superhydrophilic and Superhydrophobic Surfaces. *Langmuir* **2009**, *25*, 11822–11826.

56. Feng, L.; Zhang, Y. A.; Xi, J. M.; Zhu, Y.; Wang, N.; Xia, F.; Jiang, L. Petal Effect: A Superhydrophobic State with High Adhesive Force. *Langmuir* **2008**, *24*, 4114–4119.
57. Sheen, Y. C.; Chang, W. H.; Chen, W. C.; Chang, Y. H.; Huang, Y. C.; Chang, F. C. Non-fluorinated Superamphiphobic Surfaces through Sol−Gel Processing of Methyltriethoxysilane and Tetraethoxysilane. *Mater. Chem. Phys.* **2009**, *114*, 63–68.
58. Lai, Y. K.; Gao, X. F.; Zhuang, H. F.; Huang, J. Y.; Lin, C. J.; Jiang, L. Designing Superhydrophobic Porous Nanostructures with Tunable Water Adhesion. *Adv. Mater.* **2009**, *21*, 3799–3803.
59. Lin, P. C.; Yang, S. Mechanically Switchable Wetting on Wrinkled Elastomers with Dual-Scale Roughness. *Soft Matter* **2009**, *5*, 1011–1018.
60. Minko, S.; Muller, M.; Motornov, M.; Nitschke, M.; Grundke, K.; Stamm, M. Two-Level Structured Self-Adaptive Surfaces with Reversibly Tunable Properties. *J. Am. Chem. Soc.* **2003**, *125*, 3896–3900.
61. Mendelsohn, J. D.; Barrett, C. J.; Chan, V. V.; Pal, A. J.; Mayes, A. M.; Rubner, M. F. Fabrication of Microporous Thin Films from Polyelectrolyte Multilayers. *Langmuir* **2000**, *16*, 5017–5023.
62. Joly, S.; Kane, R.; Radzilowski, L.; Wang, T.; Wu, A.; Cohen, R. E.; Thomas, E. L.; Rubner, M. F. Multilayer Nanoreactors for Metallic and Semiconducting Particles. *Langmuir* **2000**, *15*, 1354–1359.